Hindawi
Mediators of Inflammation
Volume 2019, Article ID 6168340, 15 pages
https://doi.org/10.1155/2019/6168340

Research Article

Andrographolide Protects against HG-Induced Inflammation, Apoptosis, Migration, and Impairment of Angiogenesis via PI3K/AKT-eNOS Signalling in HUVECs

Ming-Xia Duan,[1,2,3] Heng Zhou,[1,2,3] Qing-Qing Wu,[1,2,3] Chen Liu,[1,2,3] Yang Xiao,[1,2,3] Wei Deng,[1,2,3] and Qi-Zhu Tang[1,2,3]

[1]*Department of Cardiology, Renmin Hospital of Wuhan University, Wuhan, China*
[2]*Cardiovascular Research Institute, Wuhan University, Wuhan, China*
[3]*Hubei Key Laboratory of Cardiology, Wuhan, China*

Correspondence should be addressed to Wei Deng; vivideng1982@whu.edu.cn and Qi-Zhu Tang; qztang@whu.edu.cn

Received 11 December 2018; Revised 1 April 2019; Accepted 8 May 2019; Published 7 October 2019

Academic Editor: Alex Kleinjan

Andrographolide (Andr) is a major component isolated from the plant *Andrographis paniculata*. Inflammation, apoptosis, and impaired angiogenesis are implicated in the pathogenesis of high glucose (HG)-induced injury of vascular endotheliocytes. Our study is aimed at evaluating the effect of Andr on HG-induced HUVEC injury and the underlying mechanism. HUVECs were exposed to HG levels (33 mM) and treated with Andr (0, 12.5, 25, and 50 μM). Western blot analysis, real-time PCR, immunofluorescence staining, the scratch test, and the tube formation assay were performed to assess the effects of Andr. We discovered that Andr inhibited the inflammatory response (IL-1β, IL-6, and TNFα), decreased the apoptosis ratio and cell migration, and promoted tube formation in response to HG stimulation. Andr ameliorated the levels of phosphorylated PI3K (p-PI3K), phosphorylated AKT (p-AKT), and phosphorylated eNOS (p-eNOS). The expression of vascular endothelial growth factor (VEGF) protein, a vital factor in angiogenesis, was improved by Andr treatment under HG stimulation. LY294002 is a blocker of PI3K, MK-2206 2HCI (MK-2206) is a highly selective AKT inhibitor, and L-NAME is a suppressor of eNOS, all of which significantly reduce Andr-mediated protective effects *in vitro*. Hence, Andr may be involved in regulating HG-induced injury by activating PI3K/AKT-eNOS signalling in HUVECs.

1. Introduction

Abundant evidence indicates that diabetes mellitus can cause a series of complicated pathophysiological changes including inflammation, apoptosis, autophagy, and a variety of vascular complications, which are the major risk factors for cardiovascular diseases [1, 2]. High glucose (HG), a primary independent risk factor for diabetic macrovascular disease, has been reported to play a key role in diabetes mellitus [3]. Many studies have suggested that HG not only triggers the proinflammatory response of adipose tissue in rats under a clamping environment but also causes apoptosis by increasing glucose oxidation and reactive oxygen species (ROS) levels [3, 4]. Angiogenesis is defined as the development of new blood vessels from existing capillaries or posterior capillaries through the migration and proliferation of endothelial cells. Evidence shows that HG suppresses angiogenesis due to lack of blood [5]. As the most potent angiogenic promoter, vascular endothelial growth factor (VEGF) increases vascular permeability and enhances endothelial cell proliferation to promote angiogenesis [6]. At present, the treatment of HG mainly focuses on a reasonable diet, proper exercise, and drug treatment. However, the prognosis of HG is still poor, and identifying novel therapeutic agents that inhibit inflammation and apoptosis and ameliorate endothelial dysfunction is important for HG induced injury [7].

Andrographolide (Andr) is the main effective component of the plant *Andrographis paniculata* [8]. This plant possesses various biological properties, including anti-inflammatory

Table 1: Primer sequences used for RT-PCR.

Genes (species)	Forward	Reverse
IL-1β (H)	GGCTGCTCTGGGATTCTCTT	ATTTCACTGGCGAGCTCAGG
IL-6 (H)	TTTTGGTGTTGTGCAAGGGTC	ATCGCTCCCTCTCCCTGTAA
TNFα (H)	TGGGATCATTGCCCTGTGAG	GGTGTCTGAAGGAGGGGGTA
GAPDH (H)	TTCACCACCATGGAGAAGGC	AGTGATGGCATGGACTGTGG

H: human.

[9], antioxidant [10], antihypertrophic [11], and antiapoptotic [12] activities. Recent researches have reported the antihyperglycaemic effect of Andr. Liang et al. indicated that Andr treatment ameliorated diabetic cardiomyopathy via regulating NOX/Nrf2-mediated oxidative stress and NF-κB-mediated inflammation [13]. Moreover, Andr inhibited the expression of fibronectin in diabetic nephropathy by suppressing the activation of activator protein-1 [14]. Andr inhibits HG-induced fibrosis and apoptosis and plays a protective role in murine renal mesangial cell lines [15]. The phosphoinositide 3-kinase (PI3K)/serine/threonine kinase (AKT) signalling pathway is involved in cell proliferation, migration, apoptosis, cell cycle, telomerase activity, and inflammation [16]. Extensive research has indicated that promoting PI3K/AKT signalling can suppress HG-induced inflammation [17], apoptosis [18], and impairment of angiogenesis [19]. Andr can regulate different cell types, such as rat primary hepatocytes [20] and human umbilical vein endothelial cells (HUVECs) [21], due to its ability to activate the PI3K/AKT signalling pathway. Based on these findings, we hypothesized that Andr may play a protective role in HG-induced injury by regulating PI3K/AKT signalling in HUVECs. The purpose of our study was to investigate the effects of Andr on HG-induced cell injury and the underlying mechanisms.

2. Materials and Methods

2.1. Chemicals and Reagents. Andrographolide (>98% purity) was obtained from Shanghai Winberb Medical Co. (Shanghai, China) and dissolved in a vehicle (DMSO, D2650). DMSO was purchased from Sigma-Aldrich (St. Louis, MO, United States). LY294002 (HY-10108), MK-2206 (HY-10358), L-NAME (HY-18729A), and cell counting kit (CCK)-8 were obtained from MedChemExpress (United States). The LDH and MDA assay kits were purchased from Nanjing Jiancheng Bioengineering Institute (Nanjing, China).

2.2. HUVEC Culture. The HUVEC-12 cell line (YRGene, NC006) was incubated with DMEM (1x) supplemented with 10% FBS, and the cells were cultured with 5% CO_2 at 37°C for 48 hours. HUVECs between the third and fifth passages were used in our study [22, 23]. To assess the effect of Andr on HG-induced injury of HUVECs, the cells were seeded in 6-well, 24-well, and 96-well plates for 24 hours. After 4-6 hours of starvation in a serum-free medium, the cells were treated with Andr (12.5, 25, and 50 μM) for 24/36 hours in HG (33 mM) or mannitol (MG; 27.8 mM mannitol +5.5 mM glucose). Cells were also treated with LY294002 (10 μM) to block PI3K and MK-2206 (100 nM) to inhibit AKT and L-NAME (100 μM) to suppress eNOS. After 24 hours, the cells in 6-well plates were collected for Western blots and RNA detection, the cells in 24-well plates were collected for TUNEL staining, and the cells in 96-well plates were collected for cell counting kit-8 (CCK-8) assay.

2.3. CCK-8 Assay. Cell viability was detected by the CCK-8 assay based on the manufacturer's instructions (Dojindo Molecular Technologies, Rockville, USA). HUVECs were seeded into 96-well plates at a density of 4500 cells/well. Cells were treated with Andr (12.5, 25, and 50 μM) for 6-36 hours with/without HG, LY294002 (10 μM), MK-2206 (100 nM), and L-NAME (100 μM). Then, 10 μM of CCK-8 was added to each well for 3 hours of incubation. The absorbance at 450 nm (OD450) was measured using an enzyme labelling apparatus, as described previously [11, 24, 25].

2.4. Detection of Lactate Dehydrogenase (LDH) and Malondialdehyde (MDA) Levels. LDH and MDA assay kits (Nanjing Jiancheng Bioengineering Institute, Nanjing, China) were used in accordance with the manufacturer's instructions to detect LDH and MDA activity. HUVECs were incubated in 24-well plates and treated with Andr (50 μM), LY294002 (10 μM), MK-2206 (100 nM), and L-NAME (100 μM) for 24 hours. Then, the cells were centrifuged in tubes to obtain the supernatant. The ratio of cell number to extract was 500-1000 : 1, ultrasound was used to lyse the cells, and centrifugation was performed to obtain the supernatant. The absorbance was measured at 490 nm.

2.5. Quantitative Real-Time Polymerase Chain Reaction (RT-PCR). HUVECs were seeded in 6-well plates for 24 hours. After 4-6 hours of starvation in a serum-free medium, the cells were treated with Andr (12.5, 25, and 50 μM) for 24 hours in HG DMEM (1x). Total RNA was extracted from HUVECs using TRIzol (Invitrogen, USA), and the total RNA was reverse transcribed to cDNA using a reverse transcription kit (Roche, Germany) as reported previously [26]. The Roche LightCycler480 real-time PCR instrument (Roche, Germany) was used for the amplification, and the PCR results were quantitatively analysed. The mRNA expression levels of IL-1β, IL-6, and TNFα were normalized to GAPDH gene expression. The primers used in this study are shown in Table 1.

2.6. Western Blot Analysis. HUVECs were homogenized in RIPA lysis (Wuhan Google Biological Technology Co., Ltd, China) buffer to obtain total proteins. According to the previous studies [11, 17], the protein concentrations were

measured by a BCA Protein Assay Kit (Thermo Fisher Scientific, USA) and denatured at 72°C for 10 minutes. Approximately 50 μg of protein was separated by 10% SDS-PAGE and then transferred to PVDF membranes (Millipore, USA). After incubation with the specified primary antibodies for 12 hours at 4°C and secondary antibodies for 60 minutes at homeothermy, the membranes were washed three times with TBST. Then, the blots were visualized using a two-colour infrared imaging system (Odyssey, USA). Expression levels of proteins include VEGF (1 : 1000, ab46154, Abcam), p-PI3K (1 : 1000, 4228S, CST), T-PI3K (1 : 1000, 4245, CST), p-AKT (1 : 1000, 4060, CST), T-AKT (1 : 1000, 4691, CST), p-eNOS (1 : 1000, ab195944, Abcam), T-eNOS (1 : 1000, sc-654, SANTA), Bcl-2 (1 : 1000, 2870, CST), Bax (1 : 1000, 2722, CST), C-caspase3 (1 : 1000, 9661, CST), and GAPDH (1 : 1000, 2118, CST). These proteins were normalized to GAPDH expression.

2.7. TUNEL Staining. The cultured cells were prepared and stained according to the manufacturer's instructions, and the apoptotic cells were measured by the Apoptosis Fluorescein Detection Kit (Millipore, USA). Briefly, the cells were washed 3 times with PBS and fixed in 4% paraformaldehyde for 5 minutes. Cells were treated with proteinase K (20 μg/ml) for 20 minutes and incubated with terminal deoxyribonucleotidyl transferase and deoxyuridine triphosphate for 60 minutes. Nuclei were stained with DAPI (Invitrogen, USA). The results were observed using a fluorescence microscope (OLYMPUS, Japan) and calculated using Image-Pro Plus 6.0 software (Maryland, USA).

2.8. Detection of Cell Migration and Tube Formation. The cells were seeded in 6-well plates and grew to cover the bottom of the plate. After 4-6 hours of starvation in serum-free medium, HUVECs were scraped with a 100 μl sterile micropipette tip [22]. Next, the cells were treated with Andr (50 μM), LY294002 (10 μM), MK-2206 (100 nM), and L-NAME (100 μM). Then, at 0, 12, and 24 hours, migratory cells were observed by an inverted microscope (OLYMPUS, Japan) and analysed by using by Image-Pro Plus 6.0 software (Maryland, USA).

According to the manufacturer's instructions, frozen BD Matrigel™ (Growth Factor Reduced, #356231) was melted into liquid at -4°C, and 10 μl of Matrigel was added to the bottom of each ibidi vasculogenic glass slide. After the Matrigel solidified, the cell suspension (10^4 cells/well) was added, and the cells were treated with HG for 24 hours. An inverted microscope was used to evaluate tube formation. Image-Pro Plus 6.0 software (Maryland, USA) was used to determine the number of tubes.

2.9. Statistical Analysis. All results are presented as the mean ± SEM and were analysed using SPSS 17.0 software. Comparisons between two groups were performed using an unpaired Student's t-test. One-way ANOVA was used for comparisons among three or more groups. A value of $P < 0.05$ was regarded as statistically significant.

3. Results

3.1. Andr Attenuates HG-Induced Inflammation and Apoptosis in HUVECs. HUVECs were stimulated with HG and treated with different concentrations of Andr (0, 12.5, 25, and 50 μM) for 24 hours. Four concentrations of Andr had no effect on cell viability (Figure 1(a)). Andr treatment improved the HG-induced decline of cell viability in a dose-dependent manner (Figure 1(b)). We also detected the beneficial effect of Andr at different time points (4, 6, 12, 24, and 36 hours), showing that the cell viability began to increase after 6 hours, reaching the highest level at 24 hours and remaining unchanged at 36 hours; thus, our experiment was conducted at 6-24 hours (Figure 1(c)). To evaluate the protective role of Andr under HG conditions, LDH leakage, MDA concentration, mRNA expression of inflammation biomarkers (IL-1β, IL-6, and TNFα), and apoptosis were detected in each group. The release of LDH and MDA, two indicators of HG-induced cell injury, was enhanced with HG stimulation and improved after 50 μM Andr treatment (Figures 1(d) and 1(e)). Andr inhibited HG-induced inflammatory cytokine transcription in a dose-dependent manner (Figures 1(f)–1(h)). The HG-induced increase in the apoptosis ratio in HUVECs was attenuated by Andr treatment (Figures 1(i) and 1(j)). In addition, Andr decreased the expression of the proapoptosis proteins Bax and C-caspase3 and increased the expression of the antiapoptosis protein Bcl-2 after HG stimulation (Figures 1(k) and 1(l)). These data indicated that Andr plays a protective effect in response to HG injury, including inflammation and apoptosis.

3.2. Andr Attenuates HG-Induced Cell Migration and Impairment of Angiogenesis in HUVECs. HG often leads to impaired angiogenesis [5] and promotes migration [21]. To evaluate the effect of Andr on migration and angiogenesis, we detected cell migration and tube formation in HUVECs exposed to HG with/without Andr treatment. Twenty-four hours after HG stimulation, HUVECs showed a large increase in cell migration (Figures 2(a) and 2(b)) and a decrease in tube formation (Figures 2(c) and 2(d)). Additionally, after 24 hours of treatment with Andr (50 μM), the number of migrated cells was inhibited, and tube formation was substantially improved compared to that in the HG group. We also found that the expression of VEGF, a critical factor of angiogenesis, was significantly reduced with HG exposure. However, VEGF protein expression was noticeably ameliorated after Andr treatment (Figures 2(e) and 2(f)). These data showed that Andr could restrain HG-stimulated HUVEC migration and improve tube formation.

3.3. Andr Regulates PI3K/AKT-eNOS Signalling In Vitro. To assess the underlying mechanism of Andr in HUVECs under HG conditions, PI3K/AKT-eNOS signalling was detected. As shown in Figures 3(a)–3(d), the expression of p-PI3K, p-AKT, and p-eNOS proteins was decreased after HG stimulation for 24 hours, but the expression of T-PI3K, T-AKT, and T-eNOS proteins showed no significant changes. Andr increased the levels of p-PI3K, p-AKT, and p-eNOS protein

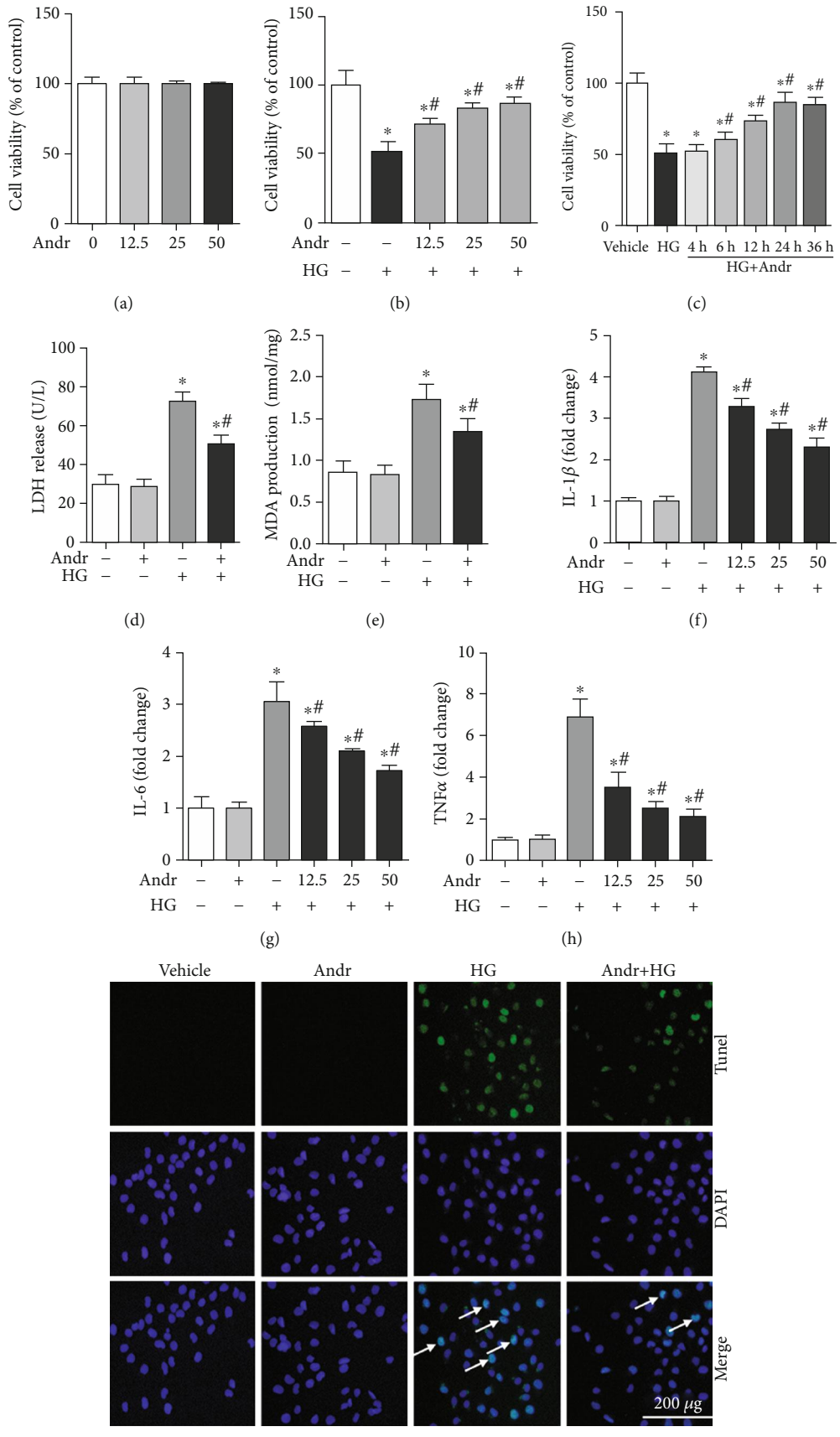

Figure 1: Continued.

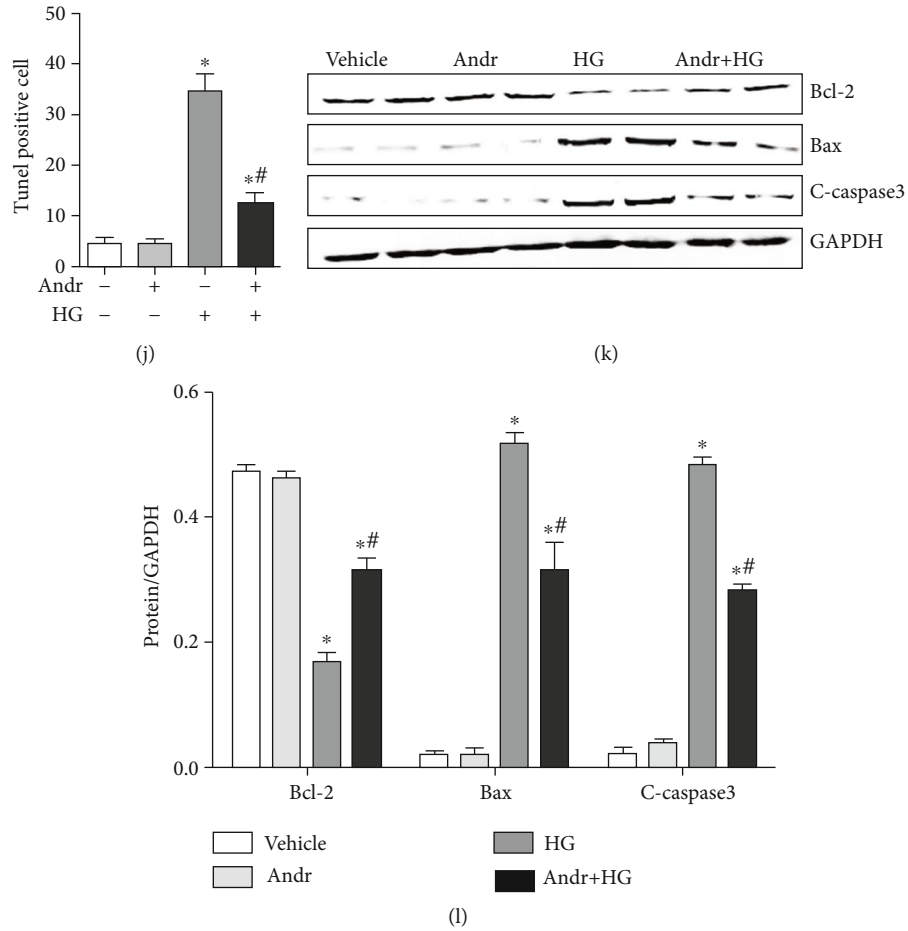

Figure 1: Andr attenuates HG-induced inflammation and apoptosis in HUVECs. HUVECs were exposed to HG (33 mM) and treated with different concentrations of Andr (0, 12.5, 25, and 50 μM) for 24/36 hours. (a, b) The cell counting kit-8 assay was used to assess cell viability in each group ($n = 6$). (c) The effect of Andr was assessed at different time points in each group ($n = 6$). (d, e) LDH leakage (d) and MDA concentration (e) in each group ($n = 6$). (f–h) The mRNA levels of IL-1β, IL-6, and TNFα in HUVECs in each group ($n = 6$). (i, j) TUNEL staining and quantitative analysis of apoptotic cells in each group ($n = 6$). (k, l) The expression of Bcl-2, Bax, and C-caspase3 protein and quantitative analysis in each group ($n = 6$). $^{*}P < 0.05$ vs. the control group. $^{\#}P < 0.05$ vs. the HG group.

and had no remarkable effects on T-PI3K, T-AKT, and T-eNOS. These data demonstrated that the protective role of Andr under HG conditions may be ascribed to the regulation of PI3K/AKT-eNOS signalling. As shown in Figures 3(e) and 3(f), LY294002 administration decreased P-PI3K levels in a dose-dependent manner (2.5, 5, 10, and 20 μM). Figures 3(g) and 3(h) demonstrate that MK-2206 treatment decreased P-AKT levels in a dose-dependent manner (25, 50, 100, and 200 nM), and Figures 3(i) and 3(j) demonstrate that L-NAME treatment decreased P-eNOS levels in a dose-dependent manner (25, 50, 100, and 200 μM). In the present study, we used LY294002 (10 μM), MK-2206 (100 nM), and L-NAME (100 μM) at the optimal concentrations.

3.4. Andr Attenuated HG-Induced Inflammation, Apoptosis, Cell Migration, and Impairment of Angiogenesis by PI3K-AKT-eNOS Signalling In Vitro. To further evaluate whether the effect of Andr relies on PI3K/AKT-eNOS signalling, we treated HUVECs with a PI3K inhibitor (LY294002), an AKT inhibitor (MK-2206), and an eNOS inhibitor (L-NAME) for 24 hours. As shown in Figures 4(b) and 4(c), HG-induced increases in LDH release and MDA production were markedly decreased in Andr-treated HUVECs, and the protective effect of Andr was significantly reduced after treatment with LY294002, MK-2206, and L-NAME. Meanwhile, in the LY294002, MK-2206, and L-NAME groups, the levels of LDH and MDA were markedly increased. Furthermore, LY294002, MK-2206, and L-NAME treatments significantly reduced the ability of Andr to enhance cell viability following HG stimulation (Figure 4(a)). Moreover, HG-induced inflammation and apoptosis, as evidenced by the increased mRNA levels of IL-1β, IL-6, and TNFα, as well as the number of apoptotic cells, were ameliorated by Andr but not by treatment with LY294002, MK-2206, and L-NAME (Figures 4(d)–4(h)). These data suggest that Andr exerts anti-inflammatory and antiapoptotic effects and may rely on the regulation of PI3K/AKT-eNOS signalling. We also performed cell migration and tube formation assays. LY294002, MK-2206, and L-NAME were used, and

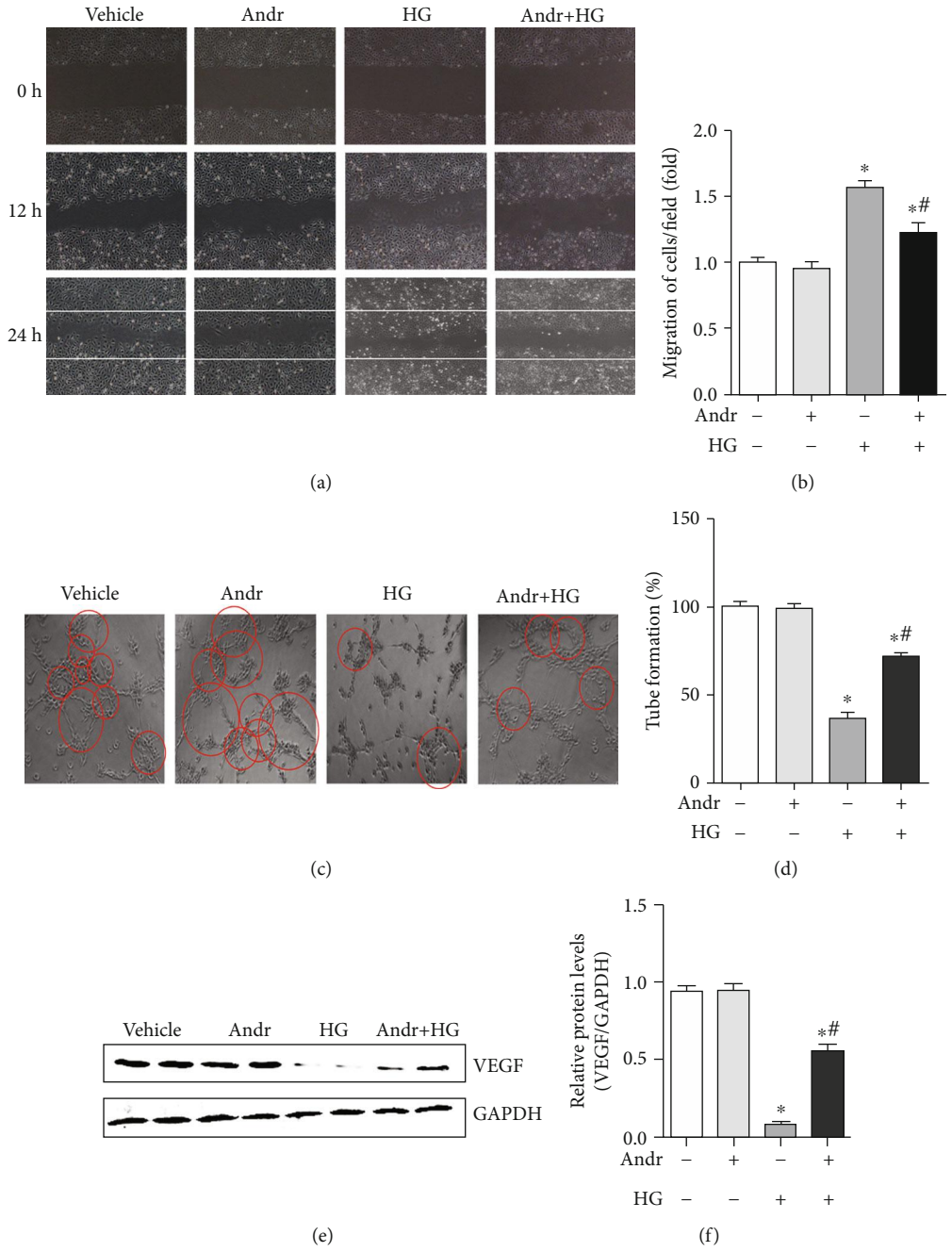

Figure 2: Andr attenuates HG-induced cell migration and impairment of angiogenesis in HUVECs. (a, b) In the scratch assay, HUVECs were treated with Andr (50 μM) and/or HG for 24 hours and photographed at 0, 12, and 24 hours ($n = 6$). (c, d) In the tube formation assay, HUVECs were treated with Andr (50 μM) and/or HG. After 24 hours, images were acquired by inverted microscopy, and the results were analysed in each group ($n = 6$). (e, f) The expression of VEGF protein and the quantitative analysis in each group ($n = 6$). $^{*}P < 0.05$ vs. the control group. $^{\#}P < 0.05$ vs. the HG group.

we observed that the number of tubes formed (Figures 4(k) and 4(l)) and the expression of VEGF (Figures 4(m) and 4(n)) were increased slightly; in addition, the number of migrated cells was decreased slightly by Andr treatment compared with that in the HG group (Figures 4(i) and 4(j)). These data indicate that the ability of Andr to protect against impaired angiogenesis and inhibit cell migration may depend on PI3K/AKT-eNOS signalling.

4. Discussion

Currently, chronic hyperglycaemia can not only directly cause injury of endothelial cells but also induce apoptosis by increasing the level of ROS and advanced glycation end products [27, 28]. An increasing number of studies have indicated that inflammation, apoptosis, and impaired angiogenesis contribute to the development of HG-induced injury

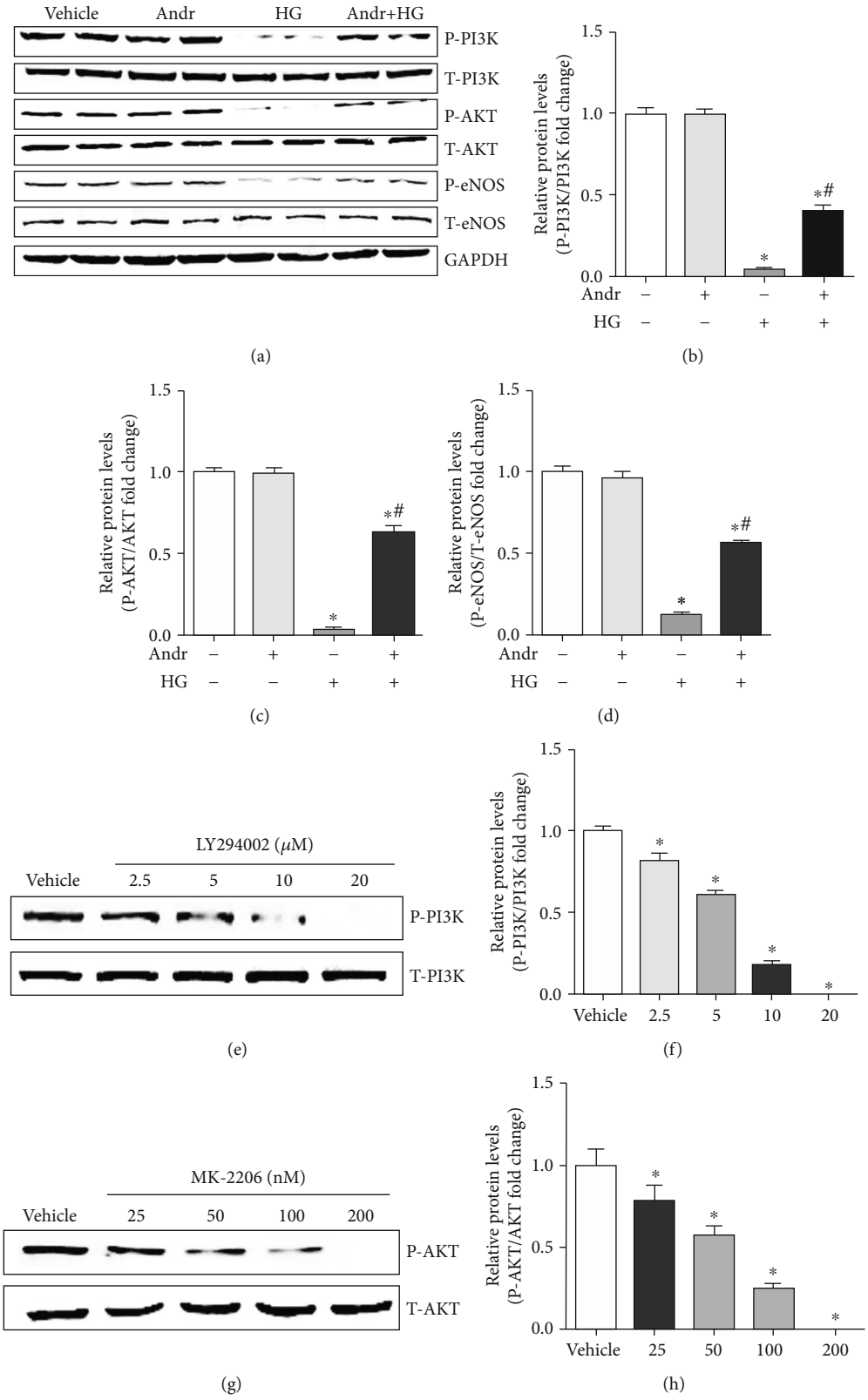

Figure 3: Continued.

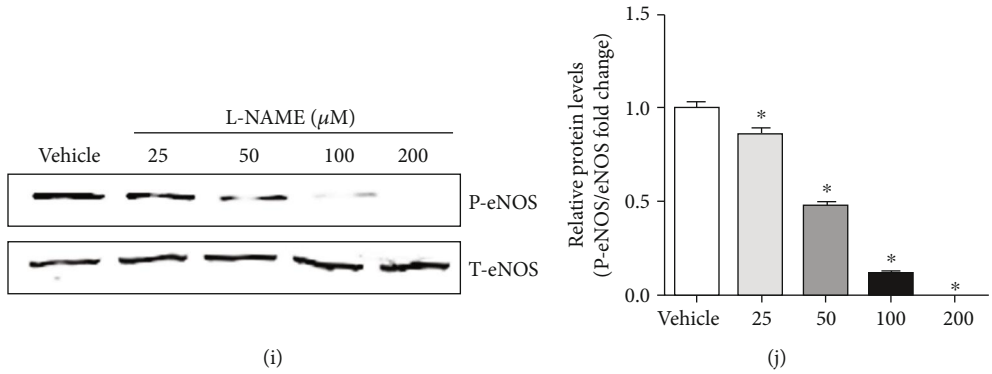

Figure 3: Andr regulates PI3K/AKT-eNOS signalling in vitro. (a) The expression of P-PI3K, T-PI3K, P-AKT, T-AKT, P-eNOS, and T-eNOS protein in each group ($n = 6$). (b–d) Quantification analysis of p-PI3K/PI3K protein, p-AKT/AKT protein, and p-eNOS/eNOS protein. (e, f) Effects of LY294002 at different concentrations on P-P13K and quantitative analysis of p-PI3K/PI3K protein ($n = 6$). (g, h) Effects of MK-2206 at different concentrations on P-AKT and quantitative analysis of p-AKT/AKT protein ($n = 6$). (i, j) Effects of L-NAME at different concentrations on P-eNOS and quantitative analysis of p-eNOS/eNOS protein ($n = 6$). $^{*}P < 0.05$ vs. the control group. $^{\#}P < 0.05$ vs. the HG group.

[2, 5]. Andr is the main ingredient extracted from the traditional herbal medicine *Andrographis paniculata*. Previous studies demonstrated that Andr pharmacologically attenuated inflammation [9], hyperglycaemia [29], cardiac hypertrophy [11], and apoptosis [12]. However, the role of Andr in HG-induced HUVEC injury remains unclarified. In the present study, we found that Andr attenuates HG-induced inflammation, apoptosis, impairment of angiogenesis, and inhibition of migration in HUVECs. The PI3K inhibitor (LY294002), AKT inhibitor (MK-2206), and eNOS inhibitor (L-NAME) were used to block PI3K/AKT-eNOS signalling, and proinflammatory cytokine (IL-1β, IL-6, and TNFα) transcription and the number of apoptotic cells were inhibited by the three suppressors cocultured with those in the HG group. Nevertheless, HUVEC migration was inhibited, while HG-induced tube formation was restored. Thus, our study suggested that Andr alleviates HG-induced HUVEC injury by activating PI3K/AKT-eNOS signalling.

Long-term hyperglycaemia in diabetes gives rise to inflammation and cell death [30]. Research has shown that inflammatory cytokines are markedly increased in animal models of diabetic cardiomyopathy [30, 31]. A previous study revealed that Andr alleviated HG-mediated inflammation through AKT/NF-κB signalling in diabetic nephropathy [10]. Moreover, the ability of Andr to attenuate cell apoptosis in high-fat diet-fed mice is due to enhanced IGF1R/PI3-K/AKT signalling [12]. In our study, Andr decreased the mRNA levels of IL-1β, IL-6, and TNFα, inhibited the number of positive apoptotic cells, and downregulated the expression of apoptosis-related proteins, which is in accordance with the previous studies [9, 10, 21]. After treatment with LY294002, MK-2206, and L-NAME, inflammation and apoptosis were slightly improved by Andr compared with those in the HG group. Additionally, cell viability began to increase after 6 hours of Andr treatment with HG stimulation, reaching the highest value at 24 hours but remaining unchanged at 36 hours, which may be partly due to the use of 10% serum in our study. A previous study indicated that the medium containing low concentrates (2, 5, or 10%) of serum did not affect cell viability under normal glucose or HG conditions after 36 hours, which is consistent with our study [25]. On the basis of these findings, Andr restores HG-induced HUVEC injury due to its anti-inflammatory and antiapoptotic activities.

Chronic hyperglycaemia causes vascular endothelial cell dysfunction, which is regarded as one of the initial markers in diabetes [32]. LDH and MDA, two markers of HUVEC injury under HG conditions, were decreased after Adnetrin-1 treatment [23]. Here, we found that Andr can reduce HG-induced LDH leakage and MDA activity. Simultaneously, it was reported that VEGF plays an important role in promoting angiogenesis including tube formation [33]. Recent available studies indicated that HG-induced suppression of tube formation and proliferation were improved through IGF1R/AKT/VEGF signalling, as well as the expression of VEGF protein [34]. Moreover, the upregulation of VEGF enhanced cardiac angiogenesis following HG exposure in rats [35]. Studies demonstrated that Andr restrained cell migration in oral cancer cells [36], renal cell carcinoma 786-0 cells [37], and human glioblastoma multiforme cells [38]. Although some reports have indicated that Andr inhibits angiogenesis, our present research demonstrated that Andr promotes angiogenesis for the following possible reasons. First, a previous study [39] suggested that proliferation, cell migration, and tube formation are decreased in HUVECs in the Andr treatment group. In our study, Andr did not affect these phenotypes or affect the expression of VEGF. Second, our results show that Andr plays a protective role under HG conditions, so there may be several underlying mechanisms: (1) HG stimulation alters the chemotactic structure of Andr and promotes the release of VEGF and (2) HG stimulation alters the response of HUVECs to Andr, leading to phenotypic changes. Finally, a previous study investigated the damaging effects of Andr on cerebral endothelial cells. Although the dosage was similar to that in our study, different cells have different reactivities to Andr, which may lead to different phenotypes. Meanwhile, previous research

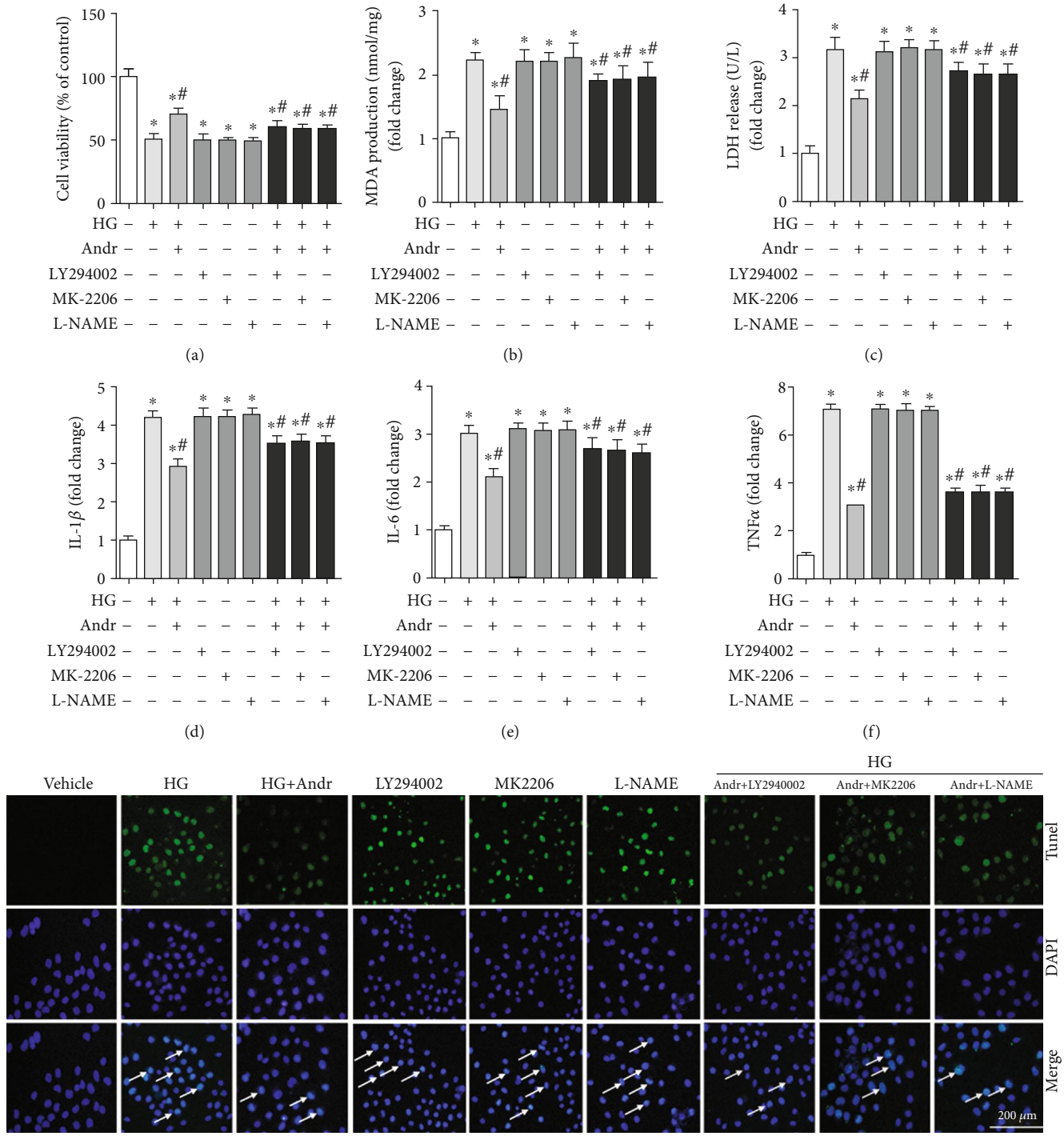

Figure 4: Continued.

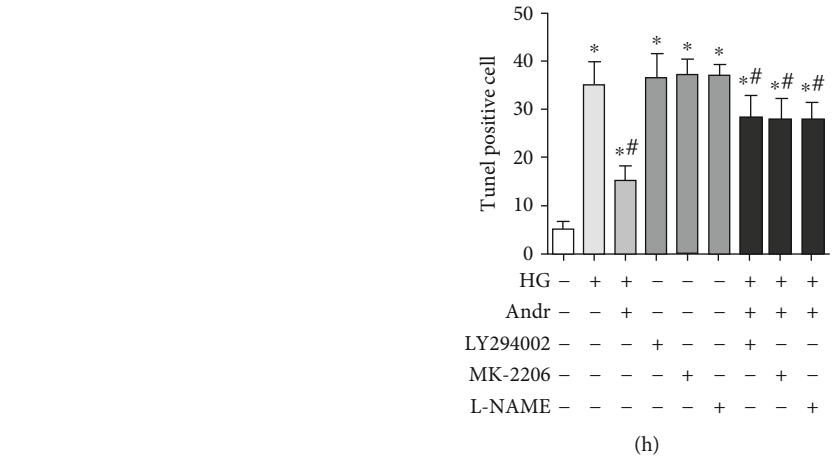

(h)

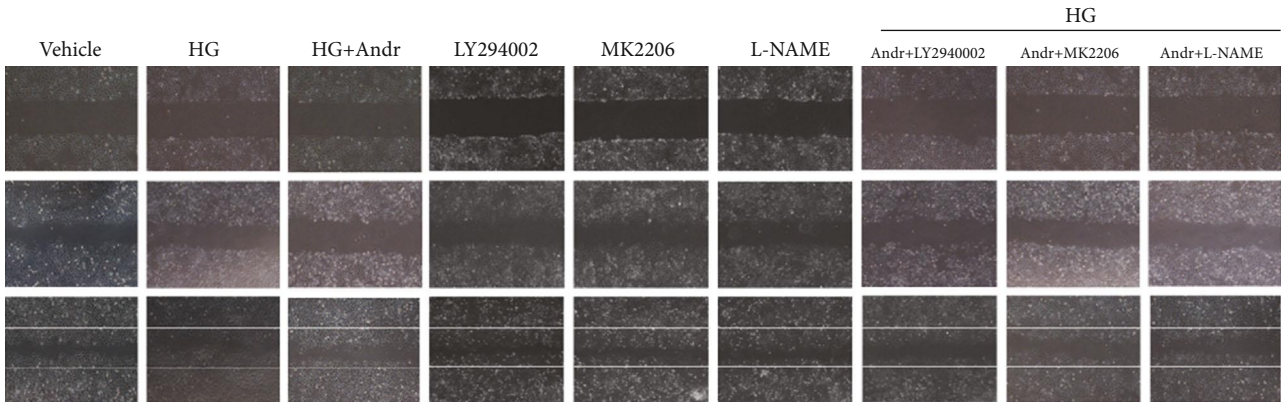

(i)

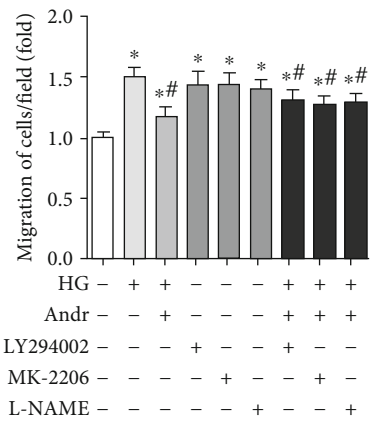

(j)

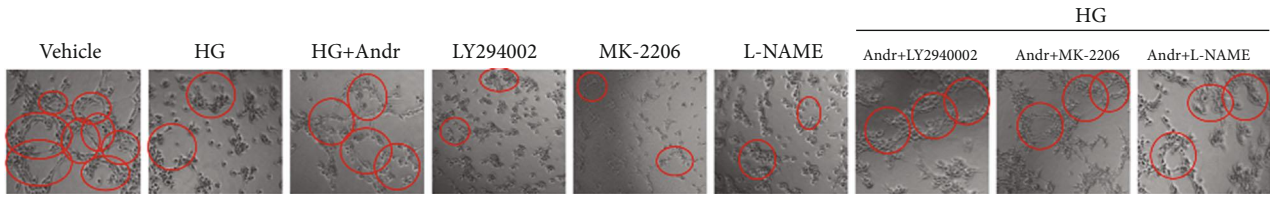

(k)

Figure 4: Continued.

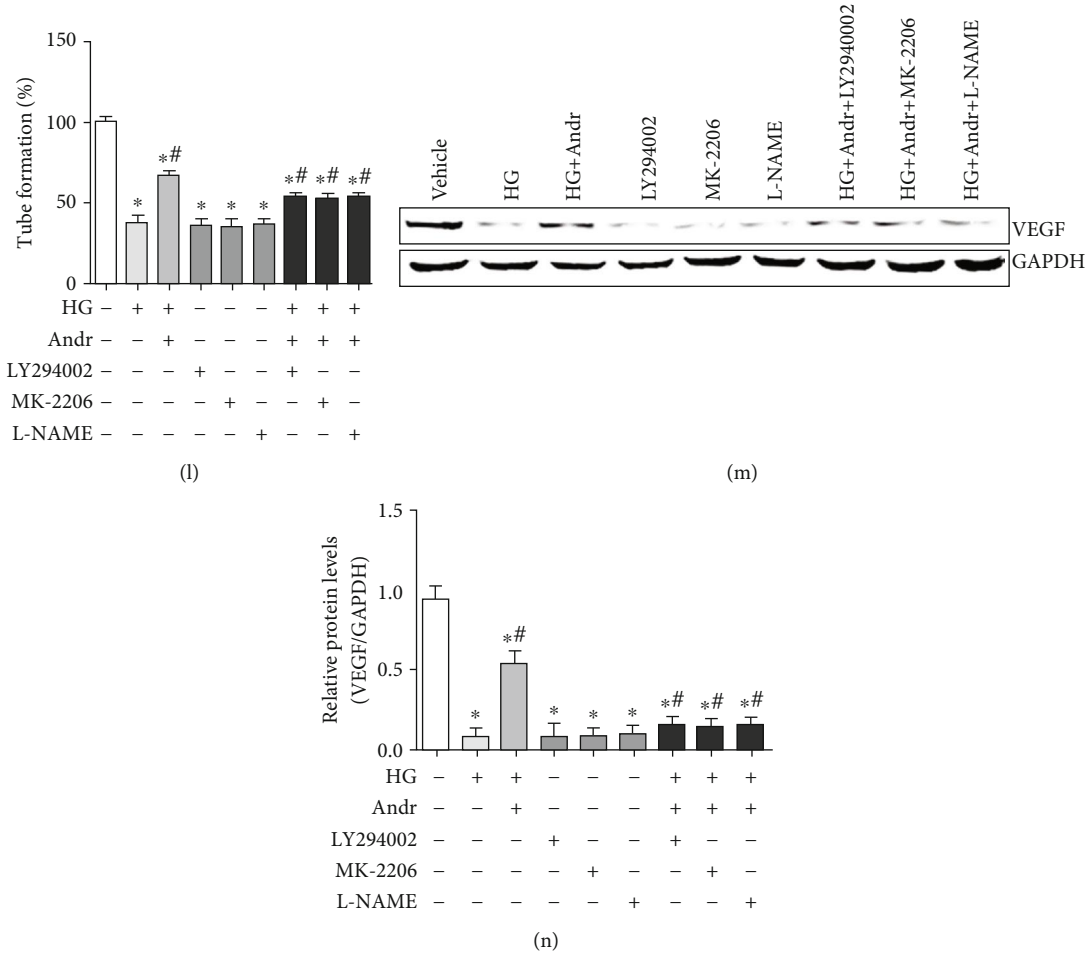

Figure 4: Andr attenuates HG-induced inflammation, apoptosis, cell migration, and impairment of angiogenesis by PI3K/AKT-eNOS signalling in vitro. HUVECs were stimulated with HG and treated with Andr (50 μM), LY294002 (10 μM), MK-2206 (100 nM), and L-NAME (100 μM) for 24 hours. (a–c) Cell viability, MDA concentration, and LDH leakage in each group ($n = 6$). (d–f) The mRNA levels of IL-1β, IL-6, and TNFα in HUVECs in each group ($n = 6$). (g, h) TUNEL staining and quantitative analysis of apoptotic cells in each group ($n = 6$). (i, j) Scratch assay and the number of migrated cells in each group ($n = 6$). (k, l) Tube formation and quantitative analysis in each group ($n = 6$). (m, n) The expression of VEGF protein and quantitative analysis in each group ($n = 6$). $^*P < 0.05$ vs. the control group. $^\#P < 0.05$ vs. the HG group.

demonstrated that with increasing Andr concentrations (5, 10, 20, 50, and 100 μM), the damage to cerebral endothelial cells becomes more serious; however, 50 μM Andr treatment exerted a protective effect on endothelial cells in our study. The reasons may be attributed to the use of different models (ischaemia/reperfusion vs. high glucose) and different cells (cerebral endothelial cells vs. HUVECs), in which Andr plays different roles. Here, we determined that Andr exerts a protective effect in HG-induced cell migration and impairment of angiogenesis, as Andr inhibited HUVEC migration, promoting tube formation, the upregulated expression of VEGF protein expression, and the downregulation of LDH and MDA levels. After being cocultured with LY294002, MK-2206, and L-NAME, Andr slightly decreased the release of LDH and MDA and cell migration ability and slightly restored tube formation ability and the levels of VEGF protein.

PI3K/AKT signalling is a central pathway that mediates various pathophysiological processes [16]. In diabetes, after the combination of insulin and growth factor receptor tyrosine kinases, PI3K is activated and generates phosphatidylinositol 3,4,5-trisphosphate, which induces the phosphorylation of AKT (p-AKT); p-AKT then activates endothelial nitric oxide synthase (eNOS) and produces NO. Hence, AKT and eNOS are considered the central factors in angiogenesis [18, 40]. The downregulation of TNFα, IL-6, and NF-κB expression was ameliorated by insulin through PI3K/AKT signalling [17]. Inactivation of the PI3K/AKT pathway led to increased positive apoptotic cells in neonatal rat cardiomyocytes [18] and prostate cancer cells [41]. Additionally, targeting VEGF leads to the inactivation of the PI3K/AKT pathway to suppress angiogenesis [19]. Moreover, epithelial-mesenchymal transition triggers the activation of PI3K/AKT signalling, which is involved in the process of hepatocellular carcinoma cell migration [42]. According to these studies, we investigated the role of Andr in PI3K/AKT-eNOS signalling after exposure to HG. Our results demonstrated that HUVECs exposed to HG had

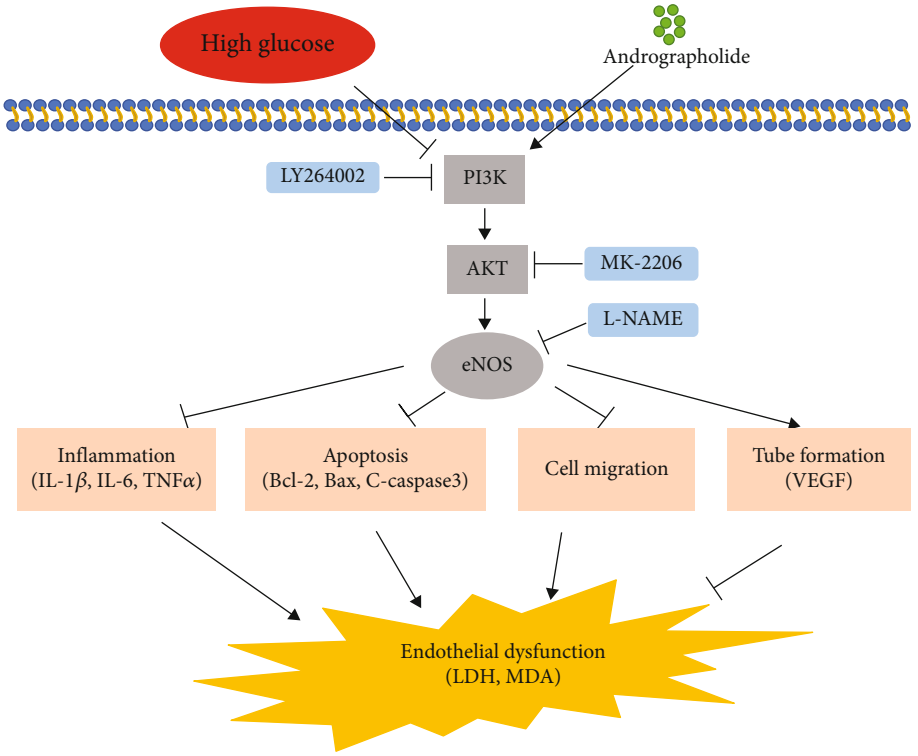

Figure 5: Graphical abstract. Andrographolide (Andr) attenuates HG-induced vascular endothelial dysfunction. Andr increases the expression of P-PI3K, P-AKT, and P-eNOS that was inhibited by HG, thus suppressing the gene expression of IL-1β, IL-6, and TNFα and the expression of VEGF. Furthermore, this effect inhibits HUVECs and promotes tubule formation, consequently decreasing the levels of LDH and MDA induced by HG.

remarkably reduced levels of p-PI3K, p-AKT, and p-eNOS protein; this effect was ameliorated by Andr treatment, which is consistent with the findings of a pervious study [20, 21]. Interestingly, the T-PI3K, T-AKT, and T-eNOS protein levels did not exhibit notable changes.

It has been reported that abnormal increases in ROS and reactive nitrogen species (RNS) induced by high glucose stimulation can damage proteins, carbohydrates, lipids, and nucleic acids, leading to oxidative/nitrosative stress. Excessive oxidation/nitrosative stress contributes to irreversible vascular injury, and HG-induced oxidative stress interferes with cell migration. This inhibition may be due to abnormal cell polarity, decreased adhesion maturity, and destabilization of protrusions [43]. In the present study, HG-induced cell migration was inhibited by Andr treatment. To the best of our knowledge, there are still significant differences in the reports of the specific mechanisms of Andr in cell migration. Andr suppresses HUVEC migration by inhibiting the expression of MMP-2 and MMP-9 [44]. Furthermore, Andr has the ability to inhibit MDA-MB-231 breast cancer cell migration by regulating nuclear factor-κB-dependent matrix metalloproteinase-9 expression [45]. Based on these data, it is reasonable to conclude that inhibition of Andr plays a protective role in HG-induced cell migration.

Alteration of endothelial cell structure and function is the pathological basis for many cardiovascular diseases, such as hypertension and diabetic cardiomyopathy. HG is a common cause of endothelial dysfunction [46, 47]. In the present study, Andr could alleviate inflammation and apoptosis induced by HG, consequently improving vascular endothelial dysfunction. Thus, Andr may delay the progression of cardiovascular diseases, reduce their mortality, and improve the quality of life of patients.

Previous studies have shown that Andr inhibits inflammation by downregulating the activity of NF-κB and NLRP3 expression [48]. Increasing the expression of STAT3 [49] and Nrf2 [50] can also make Andr play an anti-inflammatory role. Singha et al. [51] found that Andr reduces lipid peroxidation by activating the PI3K/AKT/AP-1 signalling pathway. The PI3K/AKT signalling pathway has been demonstrated to be involved in cell proliferation, migration, apoptosis, cell cycle, telomerase activity, and inflammation [16]. As shown in Figure 5, PI3K/AKT is an axis, and eNOS is a downstream of PI3K/AKT. Andr enters cells by acting on cytokine surface receptors. PI3K is activated by Andr, which further phosphorylates AKT and finally activates eNOS. Moreover, studies suggest that Andr can activate eNOS directly after it enters the cell membrane [52]. However, the specific mechanism of Andr in the PI3K/AKT-eNOS signalling pathway needs further experimental study.

5. Conclusion

In vitro, our research demonstrated that Andr attenuated HG-induced inflammation, apoptosis, migration, and

impairment of angiogenesis, via a mechanism associated with the activation of the PI3K/AKT-eNOS pathway.

Data Availability

The data used to support the findings of this study are included within the article.

Conflicts of Interest

The authors declare that they have no competing interests.

Authors' Contributions

Ming-Xia Duan, Heng Zhou, Deng Wei, and Qi-Zhu Tang contributed to the conception of the work and designed the experiments. Ming-Xia Duan, Qing-Qing Wu, and Chen Liu carried out the experiments. Ming-Xia Duan and Heng Zhou wrote and revised the manuscript. Ming-Xia Duan and Xiao Yang analysed the experimental results and revised the manuscript. Ming-Xia Duan and Heng Zhou contributed equally to this study.

Acknowledgments

This work was supported by grants from the National Natural Science Foundation of China (nos. 81700353 and 81530012), the Hubei Province's Outstanding Medical Academic Leader Programme, the China Postdoctoral Science Foundation (no. 2014M562068), the Fundamental Research Funds for the Central Universities (no. 2042017kf0060), the National Natural Science Foundation of China (81770399), and the Fundamental Research Funds for the Central Universities of China (2042018kf0121).

References

[1] H. Bugger and E. D. Abel, "Molecular mechanisms of diabetic cardiomyopathy," *Diabetologia*, vol. 57, no. 4, pp. 660–671, 2014.

[2] Z. V. Varga, Z. Giricz, L. Liaudet, G. Haskó, P. Ferdinandy, and P. Pacher, "Interplay of oxidative, nitrosative/nitrative stress, inflammation, cell death and autophagy in diabetic cardiomyopathy," *Biochimica et Biophysica Acta-Molecular Basis of Disease*, vol. 1852, no. 2, pp. 232–242, 2015.

[3] Y. Lin, A. H. Berg, P. Iyengar et al., "The hyperglycemia-induced inflammatory response in adipocytes: the role of reactive oxygen species," *Journal of Biological Chemistry*, vol. 280, no. 6, pp. 4617–4626, 2005.

[4] F. Giacco and M. Brownlee, "Oxidative stress and diabetic complications," *Circulation Research*, vol. 107, no. 9, pp. 1058–1070, 2010.

[5] P. Z. Costa and R. Soares, "Neovascularization in diabetes and its complications. Unraveling the angiogenic paradox," *Life Sciences*, vol. 92, no. 22, pp. 1037–1045, 2013.

[6] P. Carmeliet and R. K. Jain, "Molecular mechanisms and clinical applications of angiogenesis," *Nature*, vol. 473, no. 7347, pp. 298–307, 2011.

[7] H. Chen, X. Yang, K. Lu et al., "Inhibition of high glucose-induced inflammation and fibrosis by a novel curcumin derivative prevents renal and heart injury in diabetic mice," *Toxicology Letters*, vol. 278, pp. 48–58, 2017.

[8] A. Banerjee, V. Banerjee, S. Czinn, and T. Blanchard, "Increased reactive oxygen species levels cause ER stress and cytotoxicity in andrographolide treated colon cancer cells," *Oncotarget*, vol. 8, no. 16, pp. 26142–26153, 2017.

[9] Y. Li, S. He, J. Tang et al., "Andrographolide inhibits inflammatory cytokines secretion in LPS-stimulated RAW264.7 cells through suppression of NF-κB/MAPK signaling pathway," *Evidence-Based Complementary and Alternative Medicine*, vol. 2017, 9 pages, 2017.

[10] X. Ji, C. Li, Y. Ou et al., "Andrographolide ameliorates diabetic nephropathy by attenuating hyperglycemia-mediated renal oxidative stress and inflammation via Akt/NF-κB pathway," *Molecular and Cellular Endocrinology*, vol. 437, pp. 268–279, 2016.

[11] Q. Q. Wu, J. Ni, N. Zhang, H. H. Liao, Q. Z. Tang, and W. Deng, "Andrographolide protects against aortic banding-induced experimental cardiac hypertrophy by inhibiting MAPKs signaling," *Frontiers in Pharmacology*, vol. 8, p. 808, 2017.

[12] Y.-L. Hsieh, M. A. Shibu, C.-K. Lii et al., "Andrographis paniculata extract attenuates pathological cardiac hypertrophy and apoptosis in high-fat diet fed mice," *Journal of Ethnopharmacology*, vol. 192, pp. 170–177, 2016.

[13] E. Liang, X. Liu, Z. Du, R. Yang, and Y. Zhao, "Andrographolide ameliorates diabetic cardiomyopathy in mice by blockage of oxidative damage and NF-κB-mediated inflammation," *Oxidative Medicine and Cellular Longevity*, vol. 2018, 13 pages, 2018.

[14] T. Lan, T. Wu, H. Gou et al., "Andrographolide suppresses high glucose-induced fibronectin expression in mesangial cells via inhibiting the AP-1 pathway," *Journal of Cellular Biochemistry*, vol. 114, no. 11, pp. 2562–2568, 2013.

[15] M. J. Lee, Y. K. Rao, K. Chen, Y. C. Lee, Y. S. Chung, and Y. M. Tzeng, "Andrographolide and 14-deoxy-11,12-didehydroandrographolide from Andrographis paniculata attenuate high glucose-induced fibrosis and apoptosis in murine renal mesangeal cell lines," *Journal of Ethnopharmacology*, vol. 132, no. 2, pp. 497–505, 2010.

[16] D. Hamamdzic, R. S. Fenning, D. Patel et al., "Akt pathway is hypoactivated by synergistic actions of diabetes mellitus and hypercholesterolemia resulting in advanced coronary artery disease," *American Journal of Physiology-Heart and Circulatory Physiology*, vol. 299, no. 3, pp. H699–H706, 2010.

[17] H. Yan, Y. Ma, Y. Li et al., "Insulin inhibits inflammation and promotes atherosclerotic plaque stability via PI3K-Akt pathway activation," *Immunology Letters*, vol. 170, pp. 7–14, 2016.

[18] W. Yu, W. Zha, Z. Ke et al., "Curcumin protects neonatal rat cardiomyocytes against high glucose-induced apoptosis via PI3K/Akt signalling pathway," *Journal of Diabetes Research*, vol. 2016, 11 pages, 2016.

[19] H. X. Chen, X. X. Xu, B. Z. Tan, Z. Zhang, and X. D. Zhou, "MicroRNA-29b Inhibits Angiogenesis by Targeting *VEGFA* through the MAPK/ERK and PI3K/Akt Signaling Pathways in Endometrial Carcinoma," *Cellular Physiology and Biochemistry*, vol. 41, no. 3, pp. 933–946, 2017.

[20] C. Y. Lu, C. C. Li, C. K. Lii et al., "Andrographolide-induced pi class of glutathione S-transferase gene expression via PI3K/Akt pathway in rat primary hepatocytes," *Food and Chemical Toxicology*, vol. 49, no. 1, pp. 281–289, 2011.

[21] J.-H. Chen, G. Hsiao, A.-R. Lee, C.-C. Wu, and M.-H. Yen, "Andrographolide suppresses endothelial cell apoptosis via activation of phosphatidyl inositol-3-kinase/Akt pathway," *Biochemical Pharmacology*, vol. 67, no. 7, pp. 1337–1345, 2004.

[22] Q. Q. Wu, Y. Xiao, X. H. Jiang et al., "Evodiamine attenuates TGF-β1-induced fibroblast activation and endothelial to mesenchymal transition," *Molecular and Cellular Biochemistry*, vol. 430, no. 1-2, pp. 81–90, 2017.

[23] Y. Xing, J. Lai, X. Liu et al., "Netrin-1 restores cell injury and impaired angiogenesis in vascular endothelial cells upon high glucose by PI3K/AKT-eNOS," *Journal of Molecular Endocrinology*, vol. 58, no. 4, pp. 167–177, 2017.

[24] F. M. Ho, W. W. Lin, B. C. Chen et al., "High glucose-induced apoptosis in human vascular endothelial cells is mediated through NF-κB and c-Jun NH2-terminal kinase pathway and prevented by PI3K/Akt/eNOS pathway," *Cellular Signalling*, vol. 18, no. 3, pp. 391–399, 2006.

[25] R. Liu, D. Liu, E. Trink, E. Bojdani, G. Ning, and M. Xing, "The Akt-specific inhibitor MK2206 selectively inhibits thyroid cancer cells harboring mutations that can activate the PI3K/Akt pathway," *The Journal of Clinical Endocrinology & Metabolism*, vol. 96, no. 4, pp. E577–E585, 2011.

[26] L. Ibarra-Lara, E. Hong, E. Soria-Castro et al., "Clofibrate PPARα activation reduces oxidative stress and improves ultrastructure and ventricular hemodynamics in no-flow myocardial ischemia," *Journal of Cardiovascular Pharmacology*, vol. 60, no. 4, pp. 323–334, 2012.

[27] F. Westermeier, J. A. Riquelme, M. Pavez et al., "New Molecular Insights of Insulin in Diabetic Cardiomyopathy," *Frontiers in Physiology*, vol. 7, p. 125, 2016.

[28] G. Jia, V. G. Demarco, and J. R. Sowers, "Insulin resistance and hyperinsulinaemia in diabetic cardiomyopathy," *Nature Reviews Endocrinology*, vol. 12, no. 3, pp. 144–153, 2016.

[29] Y. Li, H. Yan, Z. Zhang et al., "Andrographolide derivative AL-1 improves insulin resistance through down-regulation of NF-κB signalling pathway," *British Journal of Pharmacology*, vol. 172, no. 12, pp. 3151–3158, 2015.

[30] B. Zhang, Q. Shen, Y. Chen et al., "Myricitrin Alleviates Oxidative Stress-induced Inflammation and Apoptosis and Protects Mice against Diabetic Cardiomyopathy," *Scientific Reports*, vol. 7, no. 1, 2017.

[31] M. Rajesh, P. Mukhopadhyay, S. Bátkai et al., "Cannabidiol Attenuates Cardiac Dysfunction, Oxidative Stress, Fibrosis, and Inflammatory and Cell Death Signaling Pathways in Diabetic Cardiomyopathy," *Journal of the American College of Cardiology*, vol. 56, no. 25, pp. 2115–2125, 2010.

[32] M. Joshi, S. R. Kotha, S. Malireddy et al., "Conundrum of pathogenesis of diabetic cardiomyopathy: role of vascular endothelial dysfunction, reactive oxygen species, and mitochondria," *Molecular and Cellular Biochemistry*, vol. 386, no. 1-2, pp. 233–249, 2014.

[33] B. Zhang, D. Wang, T. F. Ji, L. Shi, and J. L. Yu, "Overexpression of lncRNA ANRIL up-regulates VEGF expression and promotes angiogenesis of diabetes mellitus combined with cerebral infarction by activating NF-κB signaling pathway in a rat model," *Oncotarget*, vol. 8, no. 10, pp. 17347–17359, 2017.

[34] J. Lai, F. Chen, J. Chen et al., "Overexpression of decorin promoted angiogenesis in diabetic cardiomyopathy via IGF1R-AKT-VEGF signaling," *Scientific Reports*, vol. 7, no. 1, 2017.

[35] C. Gui, Z. Y. Zeng, Q. Chen, Y. W. Luo, L. Li, and L. L. Chen, "Neuregulin-1 promotes myocardial angiogenesis in the rat model of diabetic cardiomyopathy," *Cellular Physiology and Biochemistry*, vol. 46, no. 6, pp. 2325–2334, 2018.

[36] M. J. Hsieh, J. C. Chen, W. E. Yang et al., "Dehydroandrographolide inhibits oral cancer cell migration and invasion through NF-κB-, AP-1-, and SP-1-modulated matrix metalloproteinase-2 inhibition," *Biochemical Pharmacology*, vol. 130, pp. 10–20, 2017.

[37] B. I. Ran, D. U. Yujun, W. Wei, and C. Wang, "Effects of andrographolide in proliferation, migration and apoptosis of renal cell carcinoma 786-0 cells," *Journal of Jilin University*, vol. 44, pp. 18–23, 2018.

[38] S.-L. Yang, F.-H. Kuo, P.-N. Chen et al., "Andrographolide suppresses the migratory ability of human glioblastoma multiforme cells by targeting ERK1/2-mediated matrix metalloproteinase-2 expression," *Oncotarget*, vol. 8, no. 62, pp. 105860–105872, 2017.

[39] J. Dai, Y. Lin, Y. Duan et al., "Andrographolide Inhibits Angiogenesis by Inhibiting the Mir-21-5p/TIMP3 Signaling Pathway," *International Journal of Biological Sciences*, vol. 13, no. 5, pp. 660–668, 2017.

[40] X. T. Wang, Y. Gong, B. Zhou et al., "Ursolic acid ameliorates oxidative stress, inflammation and fibrosis in diabetic cardiomyopathy rats," *Biomedicine & Pharmacotherapy*, vol. 97, pp. 1461–1467, 2018.

[41] J. Lu, X. Chen, S. Qu et al., "Oridonin induces G2/M cell cycle arrest and apoptosis via the PI3K/Akt signaling pathway in hormone-independent prostate cancer cells," *Oncology Letters*, vol. 13, no. 4, pp. 2838–2846, 2017.

[42] K. Liu, X. Wu, X. Zang et al., "TRAF4 Regulates Migration, Invasion, and Epithelial-Mesenchymal Transition via PI3K/AKT Signaling in Hepatocellular Carcinoma," *Oncology Research*, vol. 25, no. 8, pp. 1329–1340, 2017.

[43] M. L. Lamers, M. E. S. Almeida, M. Vicente-Manzanares, A. F. Horwitz, and M. F. Santos, "High glucose-mediated oxidative stress impairs cell migration," *PLoS ONE*, vol. 6, no. 8, p. e22865, 2011.

[44] P. Pratheeshkumar and G. Kuttan, "Andrographolide inhibits human umbilical vein endothelial cell invasion and migration by regulating MMP-2 and MMP-9 during angiogenesis," *Journal of Environmental Pathology, Toxicology and Oncology*, vol. 30, no. 1, pp. 33–41, 2011.

[45] Z. Zhai, X. Qu, H. Li et al., "Inhibition of MDA-MB-231 breast cancer cell migration and invasion activity by andrographolide via suppression of nuclear factor-κB-dependent matrix metalloproteinase-9 expression," *Molecular Medicine Reports*, vol. 11, no. 2, pp. 1139–1145, 2015.

[46] F. Yi, Y. Hao, X. Chong, and W. Zhong, "Overexpression of microRNA-506-3p aggravates the injury of vascular endothelial cells in patients with hypertension by downregulating Beclin1 expression," *Experimental and Therapeutic Medicine*, vol. 15, no. 3, pp. 2822–2850, 2018.

[47] G. Jia, A. Whaley-Connell, and J. R. Sowers, "Diabetic cardiomyopathy: a hyperglycaemia- and insulin-resistance-induced heart disease," *Diabetologia*, vol. 61, no. 1, pp. 21–28, 2018.

[48] S. Peng, J. Gao, W. Liu et al., "Andrographolide ameliorates OVA-induced lung injury in mice by suppressing ROS-mediated NF-κB signaling and NLRP3 inflammasome activation," *Oncotarget*, vol. 7, no. 49, pp. 80262–80274, 2016.

[49] D. Yang, W. Zhang, L. Song, and F. Guo, "Andrographolide protects against cigarette smoke-induced lung inflammation

through activation of heme oxygenase-1," *Journal of Biochemical and Molecular Toxicology*, vol. 27, no. 5, pp. 259–265, 2013.

[50] W. S. D. Tan, H. Y. Peh, W. Liao et al., "Cigarette Smoke-Induced Lung Disease Predisposes to More Severe Infection with Nontypeable *Haemophilus influenzae*: Protective Effects of Andrographolide," *Journal of Natural Products*, vol. 79, no. 5, pp. 1308–1315, 2016.

[51] P. K. Singha, S. Roy, and S. Dey, "Protective activity of andrographolide and arabinogalactan proteins from Andrographis paniculata Nees. against ethanol-induced toxicity in mice," *Journal of Ethnopharmacology*, vol. 111, no. 1, pp. 13–21, 2007.

[52] C.-H. Yang, T.-L. Yen, C.-Y. Hsu, P.-A. Thomas, J.-R. Sheu, and T. Jayakumar, "Multi-targeting andrographolide, a novel NF-κB inhibitor, as a potential therapeutic agent for stroke," *International Journal of Molecular Sciences*, vol. 18, no. 8, p. 1638, 2017.